Geomagnetic and Albedo Studies with a Čerenkov Detector at 40° Geomagnetic Latitude*

J. R. WINCKLER AND K. ANDERSON
University of Minnesota, Minneapolis, Minnesota
(Received September 9, 1953)

A Čerenkov detector consisting of a Lucite radiator optically sealed to a large-area side-window photomultiplier has been flown at $\lambda=40°$ at a depth of 25 g/cm² below the top of the atmosphere. The albedo was determined and is not more than 5 percent of the incident flux for particles of $\beta>0.7$ in any upward direction. The albedo observed is too small to account for the factor-of-two difference between the observed E–W asymmetry and that predicted from the primary spectrum and geomagnetic theory. Direct asymmetry measurements by the Čerenkov counter suggest that the earth shadow cone cutoff may start at larger zenith angles than theoretically predicted. A very rough relative abundance measurement of H:He:Li gives 1:0.08:0.02.

I. INTRODUCTION

THE present investigation is concerned with two discrepancies which have arisen from high-altitude cosmic-ray measurements. The first factor is the failure of the azimuthal effect at high altitudes of the total cosmic radiation to agree via the geomagnetic theory with the measured latitude effect. The other discrepancy is the failure of the total energy, computed on the basis of the incident particle flux and geomagnetic theory, to agree with the total energy measured by the atmospheric-ionization data.

The first discrepancy appeared as a result of a latitude survey at balloon altitudes[1] and also appears in data obtained with rockets above the atmosphere.[2,3] As pointed out in Table IV, reference 1, if one compares the east-west effect at a number of latitudes with the expected effect, using the vertical counting rate *vs* latitude and also using geomagnetic theory, one finds that the measured east-west effect is about one-half the predicted value. This comparison is independent of the nature of the primary radiation, except that it is assumed to be entirely positively charged, as the comparison is made entirely on the basis of the dimensionless Störmer variable in place of the energy. As was pointed out, the azimuthal effect might be decreased by the presence of splash albedo produced by primary particles incident on the atmosphere whose secondaries then went out again and were counted as primaries by the Geiger telescopes. In order to reduce the east-west effect enough by this means to make it consistent with the measurements, it was calculated that at $\lambda=0$, 33 percent, at $\lambda=20$, 25 percent, and at $\lambda=40$, 45 percent of the western flux at 60° zenith, would have to be projected out again in the eastern direction.[1] Presumably, that part of the splash albedo which consists of stable particles would leave the atmosphere, and if it had an energy less than the cut-off energy for entrance from infinity, according to geomagnetic theory, the particles would remain trapped in the earth's field and eventually would return to the earth. It has been pointed out by Treiman,[4] that if one considers the first integral of the Störmer theory, particles leaving in the vicinity of latitude λ, and fulfilling the condition that they do not escape to infinity and therefore constitute part of the albedo, would return to the earth close to that same latitude, or to the corresponding latitude in the opposite hemisphere over wide limits of the angle of emission X. This can be seen from the Störmer first integral

$$\alpha=-R\cos\lambda\cos X+(1/R)\cos^2\lambda, \qquad (1)$$

with the auxiliary conditions that $\alpha\geq 2$, $R\leq 1$. One should note that the angle of return of the albedo particle is not the same, in general, as the angle of departure. If one, however, measures the amount of radiation leaving the atmosphere or moving in an outward direction, one can then compute the magnitude of the effect.

Evidence for albedo above the atmosphere comes from rocket range-ionization measurements of Perlow and co-workers[5,6] in which it was shown that there is an appreciable amount of low-energy radiation, possibly electrons, above the atmosphere. Van Allen, Singer, and co-workers have also shown that the ratio of the omni-directional flux to vertical telescope flux values at a number of latitudes demonstrates that the average omni-directional value is higher than the vertical, whereas, according to theory, it should be lower if all the particles measured are primaries. Measurements with telescopes in rockets by this group at various zenith angles above the atmosphere support this conclusion by an increase in the flux towards the horizontal direction. It is somewhat difficult to assess the effects of these results on the balloon measurements near the top of the atmosphere at roughly 15 g/cm². The balloon equipment used to measure the asymmetry contained 3 cm of lead in the telescope plus the counter wall

* This work supported by the joint program of the U. S. Atomic Energy Commission and the U. S. Office of Naval Research.
[1] Winckler, Stix, Dwight, and Sabin, Phys. Rev. **79**, 656–669 (1950).
[2] J. A. Van Allen and A. V. Gangnes, Phys. Rev. **78**, 50 (1950); **79**, 51 (1950).
[3] S. F. Singer, Phys. Rev. **77**, 729 (1950); **80**, 47 (1950).
[4] S. Treiman, Phys. Rev. **91**, 432 (1953).
[5] G. J. Perlow and J. D. Shipman, Jr., Phys. Rev. **71**, 325 (1947).
[6] Perlow, Davis, Kissinger, and Shipman, Phys. Rev. **88**, 321 (1952).

thickness, which gave 36 g of lead equivalent or 19 g of air equivalent. At a 60° zenith angle there were 30 g/cm² of air above the equipment, which means that the total initial energy of a proton coming downward toward the telescope must have been 270 Mev or more to be detected, or when the proton reached the telescope it had to have 112 Mev remaining. These energy values are considerably above the threshold to which the rocket measurements were sensitive, particularly the single-counter rocket values, which go down to the order of a few Mev, so that almost certainly a large amount of extra radiation was measured in some of the rocket experiments not directly relevant to the balloon data. The above-the-atmosphere splash albedo may be more intense than that observed at 15- to 25-g/cm² depth, as the primary flux is larger in directions near the horizontal as one goes to smaller and smaller depths, and these primaries are more effective in producing albedo.

The second discrepancy which has been referred to comes from a comparison of the vertical telescope balloon or rocket data with the ionization measurements of Neher,[7] in which it is generally agreed that the flux calculations, although agreeing with the ionization data in the *form* of the primary-energy spectrum, give about twice the amount of incident energy. Energy is calculated from the balloon or rocket flux measurements by the equation

$$E(\lambda)=\int_{E_{\min(\lambda)}} N(E)EdE. \qquad (2)$$

The spectrum $N(E)$ is obtained over the geomagnetically sensitive region from the vertical balloon flux measurements and is extended to higher energies using the very high energy data obtained from the air showers, which in general agree in form with the high-energy spectra obtained by other means. The errors involved in this calculation cannot account for the factor-of-two differences, except for the uncertainty in the primary flux itself, which might arise from the albedo. It was therefore considered important to make measurements of the albedo at balloon altitudes and to study the possible effect of the albedo on the two discrepancies.

II. THE ČERENKOV DETECTOR

Preliminary attempts to detect the albedo using a lead-absorption method gave a nul result at $\lambda=55°$ at 20-g/cm² atmospheric depth.[8] In these measurements a large block of lead was alternately moved to and away from the lower side of a counter telescope, and the counting rates compared. There were obviously present showers from the equipment which changed with the position of the lead block, but, nevertheless, the effect observed was essentially zero.

[7] H. V. Neher, Phys. Rev. **83**, 650 (1951).
[8] J. R. Winckler, Phys. Rev. **85**, 1053–1054 (1952).

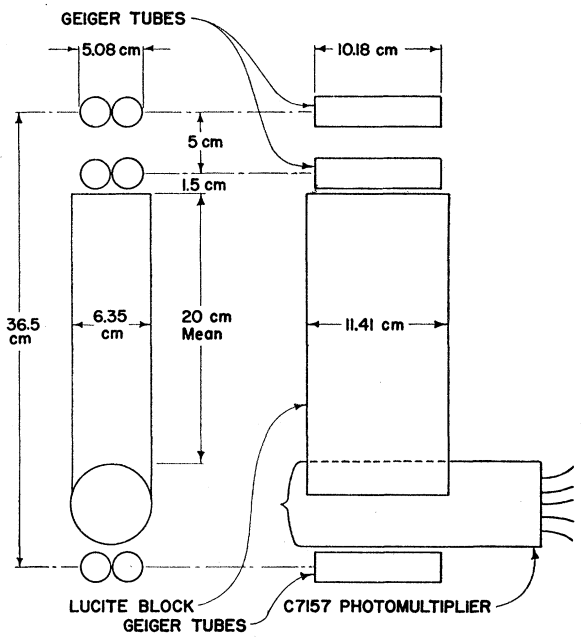

FIG. 1. Schematic diagram of the Čerenkov detector. The solid angle is 1.86 sterad-cm². The total detector stopping power is 30 g/cm².

The next experiment involved the use of a Čerenkov detector,[8] which in a preliminary form gave a small effect of upward relativistic particles at the top of the atmosphere at $\lambda=55°$. This early detector used an end-window photomultiplier tube optically connected to a side arm of a block of Lucite, which constituted the radiator. The device had strong directional properties but very poor light-collection efficiency, and was discarded in favor of a much-improved detector.[9] This detector is shown in Fig. 1 and consists of a block of Lucite to which is optically joined an RCA-type C-7157 developmental phototube. This phototube has a side window of 13 sq in. sensitive area, and four of these phototubes were obtained through the kindness of the U. S. Navy Department, Bureau of Ships. Of the original four, one was furnished with a cracked base, and one was lost because of the failure of a balloon during flight. The other two were flown successfully and results are reported in this paper.

The theory of the Čerenkov effect on a classical basis has been given by Frank and Tamm[10] following the original discovery in 1934 by Čerenkov.[11] In Fig. 2 is plotted the function $F(\beta,n)$, giving the relative number of quanta emitted for the case of Lucite, for a singly charged particle. The absolute number of quanta is obtained by multiplying $F(\beta,n)$ by $Z^2\Delta\omega t/137c$, where $\Delta\omega$ is the angular frequency region and t the thickness

[9] J. R. Winckler and K. Anderson, Rev. Sci. Instr. **23**, 765–66 (1952).
[10] I. Frank and I. Tamm, Compt. rend. acad. sci. U.R.S.S. **14**, 109 (1937).
[11] P. A. Čerenkov, Compt. rend. acad. sci. U.R.S.S. **8**, H51 (1934); Phys. Rev. **52**, 378 (1937).

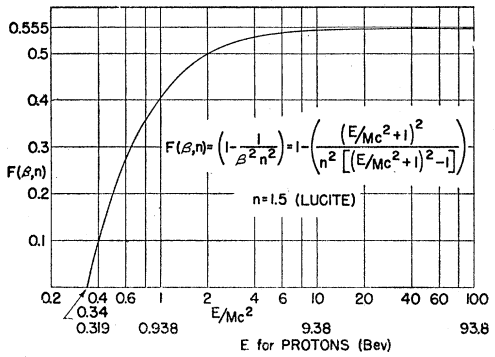

FIG. 2. Classical relative rate of quanta emission for Lucite. Absolute number of quanta $= F(\beta,n)\cdot 2\pi\Delta\lambda l Z^2/(137\lambda^2)$ in the wavelength interval $\Delta\lambda$ for thickness t cm.

in cm. The energy loss, like ionization loss, varies as the square of the particle charge Z. It is seen also that the Čerenkov threshold for Lucite occurs at a ratio of kinetic energy to rest energy of 0.34, which for protons is 0.319 Bev. The quanta emitted per cm then increases and becomes constant at about 10 times the rest energy. Considering the spectral response of the C-7157 photomultiplier, roughly 5000 usable quanta should be produced in the Lucite block by a very high energy, singly charged particle. The angle of emission θ also depends on the ratio of kinetic energy to rest energy of the particle, and reaches the limiting value of 48° for Lucite (see Fig. 3). This means that the radiation given out by a particle traversing the block from end to end will be almost entirely internally reflected and will proceed down the block in the direction of the particle. If this light is incident on the photo surface at the end, the pulse of light is recorded. If the particle proceeds the other way through the block, the light is absorbed in the blackened end and does not record. It has been pointed out by Huybrechts and Schönberg[12] that a correction term must be inserted in the classical formula to take into consideration the decreased emission in the high-frequency Čerenkov bands due to quantum-mechanical effects near the trajectory of the particles.

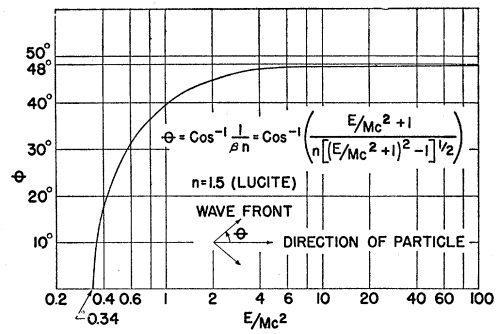

FIG. 3. Angle of emission of Čerenkov radiation for Lucite.

[12] M. Huybrechts and M. Schönberg, Nuovo cimento **9**, 764 (1952).

Because Lucite has no absorption bands in the spectral response region of the photomultiplier, it appears that this correction does not influence the calculation for Lucite. It is evident that collision electrons produced in the Lucite block by the high-energy particle may themselves give Čerenkov radiation, if they are above the threshold. The calculation of this effect shows that for high-energy, singly charged particles, there will be an increase in the total quanta produced of about 10

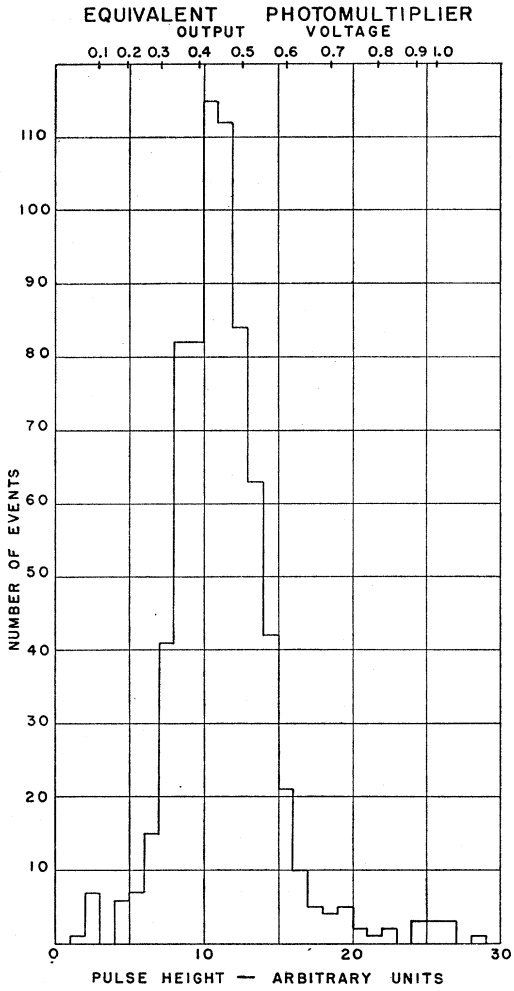

FIG. 4. Pulse-height distribution for sea-level mesons on equipment for flight E. Flight L gives very similar results.

percent and that this will add a tail to the pulse-height distribution on the high side. A typical pulse-height distribution for sea-level mesons is shown in Fig. 4. The mesons were required to traverse 6 inches of lead after passing through the Lucite block. The distribution was obtained for the tube used in flight E, referred to later, and has a half-width of about 50 percent, which is about twice that reported earlier.[9] The half-width appears to be sensitive to the photomultiplier itself, but the exact cause of the change in half-width has not been deter-

mined. This curve clearly shows a tail on the high-energy side associated with the collision electrons produced in the block.

The use of a Čerenkov detector for cosmic rays was first reported by Jelly[13] and was used by Duerden and Hyams[14] in an attempt to separate masses of slow particles. The ability of the Cerenkov detector to discriminate masses was also pointed out by one of us,[8] and comes from combining the Čerenkov emission characteristic, Fig. 2, with, say, a range determination on the particle. With the present instrument a proton of energy between 210 and 319 Mev can penetrate the block of Lucite, the phototube, and the associated Geiger counters, without producing Čerenkov radiation, which is not possible for an electron or a meson. The mass discrimination, however, is confined to a narrow energy region. The angle of emission of the radiation so far has not been utilized to advantage in cosmic-ray

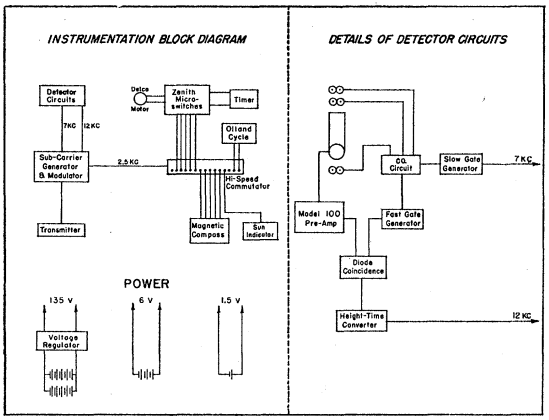

FIG. 5. Block diagram of Čerenkov detector and associate circuitry for use in the high-altitude albedo and geomagnetic studies.

experiments, because the large solid angle necessary to accumulate statistics makes the angular resolution poor; but in the case of an accelerator, one may use the angle of emission to get a very precise measurement of the beam energy, as has been demonstrated by Mather[15] and Marshall.[16] The latter also has utilized the Čerenkov radiation for very high speed counting devices because of the nature of the radiation itself. An attempt was made by Bianchi and Manducci[17] to measure the intensity as a function of energy to reproduce the classical curve, Fig. 2, using a range type of energy selector for sea-level mesons. The results seem to show a rise in the relativistic region above that predicted by classical theory. There has been no further verification of this work.

[13] J. V. Jelly, Proc. Phys. Soc. **A64**, 82 (1951).
[14] T. Duerden and B. D. Hyams, Phil. Mag. **43**, 717 (1952).
[15] R. L. Mather, Phys. Rev. **84**, 181 (1951).
[16] J. Marshall, Phys. Rev. **86**, 685 (1952).
[17] A. M. Bianchi and C. Manducci, Nuovo cimento **9**, 861 (1952).

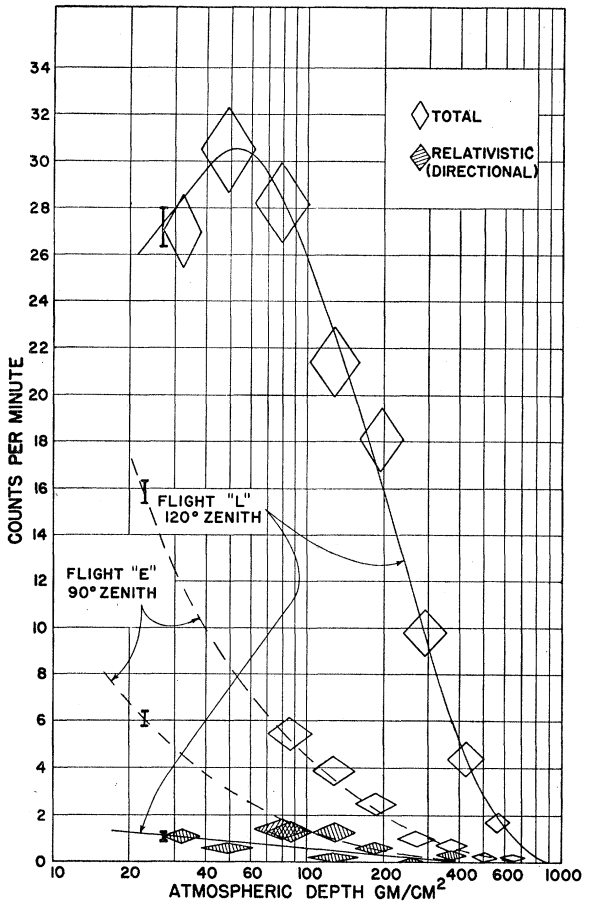

FIG. 6. Total and relativistic counting rates at 90° and 120° as a function of atmospheric depth.

III. EXPERIMENTAL DETAILS

The Čerenkov detector (Fig. 1) consists of the $2\frac{1}{2}$-in. $\times 4\frac{1}{2}$-in. $\times$ 8-in. Lucite block with one end cut to a $1\frac{1}{4}$-in. radius concave to fit the C-7157 photomultiplier. An optical seal is made with Canada balsam. The opposite end of the Lucite is painted black to absorb all incident radiation. The detector is aligned in a threefold Geiger telescope composed of 3 pairs of tubes of 4-in. sensitive length and 1-in. diameter, with the extremities $14\frac{1}{2}$ in. center-to-center. The solid angle is 1.86 sterad-cm^2. This telescope has a relatively small solid angle as necessitated by the phototube size, and long flights are necessary to accumulate meaningful directional data.

TABLE I. Level flight counting rate values.

		Pressure g/cm²	Counts/minute 0°	180°
Total	Flight *E*	23.6	20.8±.5	20.2
	Flight *L*	27.6	27.2	27.1
Relativistic	Flight *E*	23.6	17.4	1.1
	Flight *L*	27.6	21.4	1.4

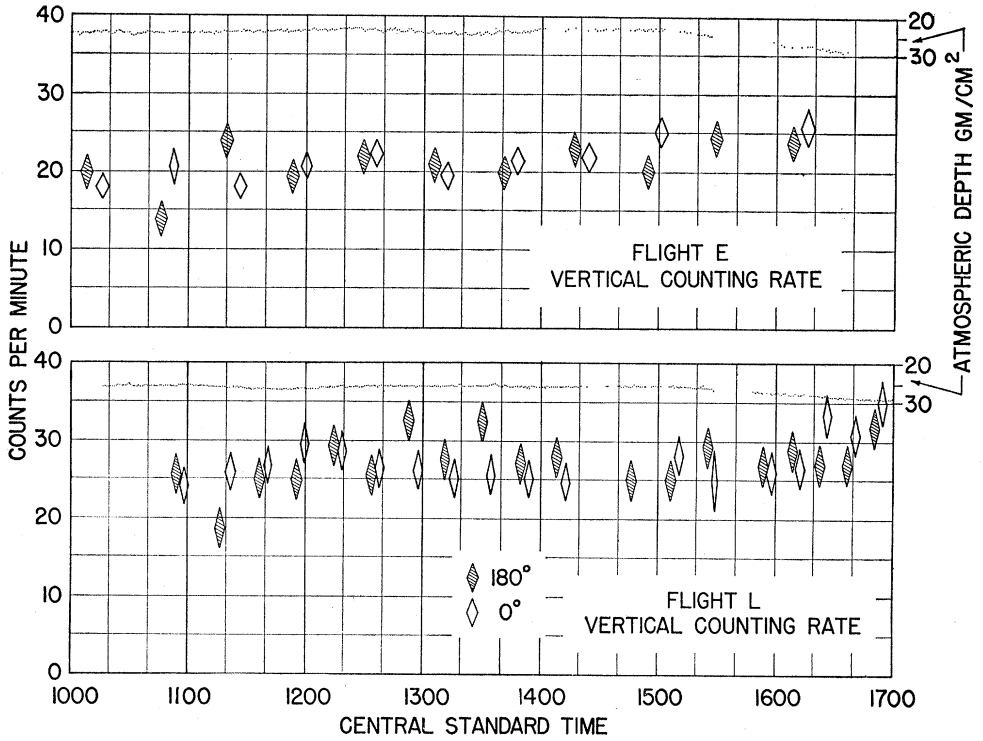

FIG. 7. Total vertical counting rate and balloon pressure height for the two flights. Data are taken for the 0° and 180° zenith positions for all events registering a Geiger telescope coincidence. The graph at the top is the balloon pressure-time record with pressure scale at right top in g/cm². Flux (particles/cm² sec sterad) = (counts/min)×0.009.

All data are given in counts/minute, which, when multiplied by 0.009, gives the flux in particles/cm² sec sterad. The total detector stopping power is 30 g/cm².

The electronics and circuit details are shown in Fig. 5. The Čerenkov pulse appears at a level of about 0.2 volt and 1 μsec in length for a singly charged, fast particle and is amplified 30 times by the model-100 preamplifier. This pulse enters the height-time converter, provided the fast gate is actuated by a signal from the Geiger telescope, and is converted into a square wave of length from 5 to 100 milliseconds. This square wave is transmitted by one of the telemetering subcarriers. The fast-gate signal is also transmitted as a suitable square wave 50 milliseconds in length on a second subcarrier. The detector is mounted so that the zenith position can be varied from straight up to straight down in steps located at 0°, 60°, 90°, 120°, and 180°, and programmed so that approximately 5 minutes are spent successively at each position. The complete gondola is also rotated about a vertical axis one turn every ten minutes. Compass readings and a sun reference photocell index the azimuth, and these data, together with the zenith position and balloon pressure height, are multiplexed on the third telemetering subcarrier. At the ground receiving station the square waves are integrated and the pulses recorded by photographing two cathode-ray tubes. The multiplexed data is displayed and photographed simultaneously on a third cathode-ray tube. Thus the Čerenkov pulse height may be recorded for every Geiger telescope event, and may be associated with the relevant direction in space indicated by the compass and zenith positions. The system is quite similar to that used previously for transmitting telescope and directional data.[1]

Two good flights, designated E and L, were obtained at $\lambda=40°$ with separate gondolas. Flight E remained level at 23 g/cm² for about 6 hours, and flight L at 27 g/cm² for a similar time. Flight E could record a pulse-height range just up to the α-particle region at four times the pulse height of a singly charged particle, and on the ascending portion the zenith angle was set at 90°. Flight L could record pulses ten times that of a singly charged particle, which made it capable of detecting the Li component. Flight L ascended through the atmosphere in the 120° zenith position, to observe the atmospheric-depth dependence of the oblique-upward component.

IV. EXPERIMENTAL RESULTS

A. Atmospheric-Depth Variation

The data obtained on ascent in the two flights are shown in Fig. 6. The total Geiger telescope flux at 120° (or 60°) passes through a maximum and drops toward

small depths. However, telescope events accompanied by a detectable Čerenkov pulse, indicating a particle having $\beta > 0.7$ moving upward 30° above the horizontal, increase slowly to about 5 percent of the total. At 90° the situation changes markedly, where the relativistic component is a much larger fraction of the total. The total flux in this case does not seem to pass through a maximum, and constitutes a little more than half the 120° (or 60°) total. The values in Fig. 6 are averaged over 360° of azimuth.

B. Vertical Data at Ceiling Altitude

The total vertical (0° or 180°) counting rate for the two flights as a function of time is shown in Fig. 7. As can be seen, the 0° and 180° rates are equal on the average, and are constant with time for most of the flight. Near the end the rate increases somewhat, which is associated with both a slight increase in depth and a northerly component of balloon drift. The average values are summarized in Table I, which also separates out the relativistic component in the 0° and 180° directions. The relativistic flux extrapolated linearly with pressure to 15 g/cm² gives 0.08/cm² sec sterad, in good agreement with values obtained previously at $\lambda = 40°$.[1]

In Fig. 8 is presented the 0° and 180° zenith pulse-height distributions for flight E at 23.6 g/cm² for full range of the equipment. The dotted curve shows the distribution obtained for sea-level mesons penetrating 6 inches of Pb after the detector. A very similar set of curves is obtained for flight L at 27.6 g/cm² (Fig. 9) for the region near the singly charged particle peak. In both cases the high altitude curve for 0° is filled out above the sea-level curve on the low pulse-height side. There is also a fraction of events for which a particle traversal is recorded but for which *no* Čerenkov pulse is observed. These extra pulses are due to particles which are able to penetrate the block but which give Čerenkov radiation between the threshold and the maximum value. The velocity is then determined and corresponds to $0.34 < E/mc^2 < 4$. In accordance with the discussion in Sec. II, this fraction is assumed to be protons with $210 < E < 319$ Mev, or upward relativistic particles. The 180° distribution shows no peak at all, but indicates a small number of upward moving particles with $0.34 < E/mc^2 < 4$, and a large number of events giving no Čerenkov light. Most of these are the downward particles recorded in the 0° direction, the remainder the protons with $210 < E < 319$ Mev for which direction is not determined. From these data the up-and-down relativistic and the lower-energy proton flux may easily be computed. The Čerenkov light output increases so

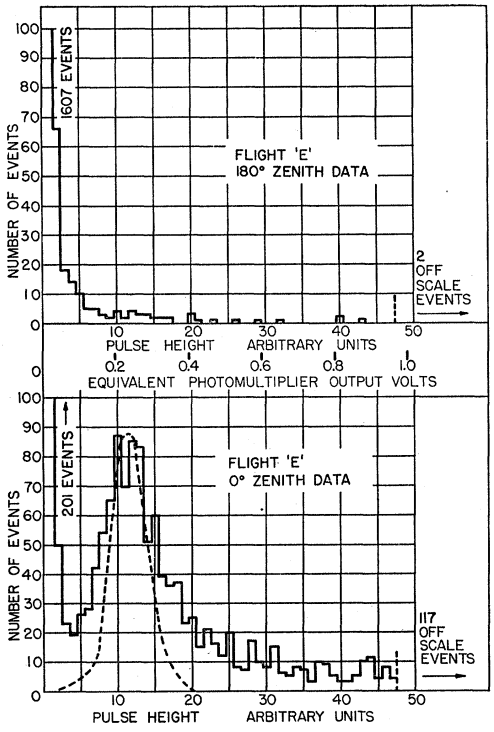

FIG. 8. Čerenkov pulse-height distributions for flight E, 0° and 180° direction at 23.6 g/cm². The dotted curve is for sea-level mesons.

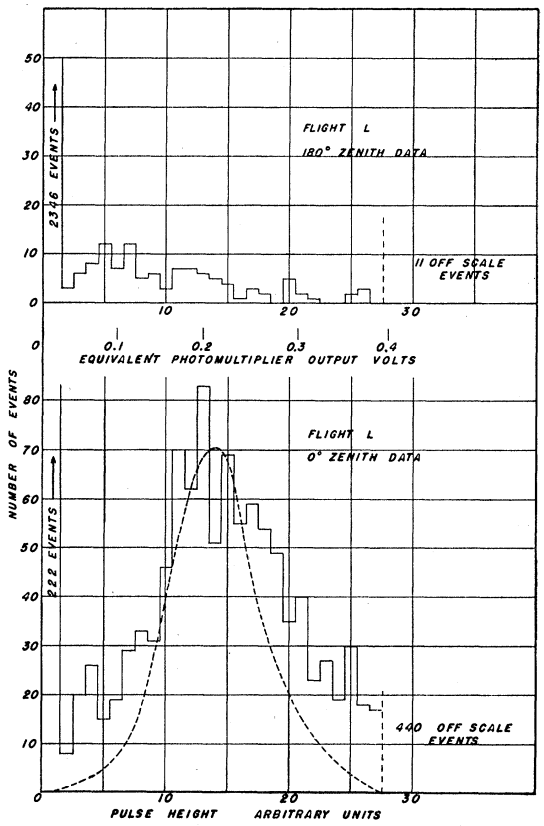

FIG. 9. Čerenkov pulse-height distributions for flight L, 0° and 180° direction at 27.6 g/cm². The dotted curve is for sea-level mesons. This is a magnified portion of full scale around proton peak.

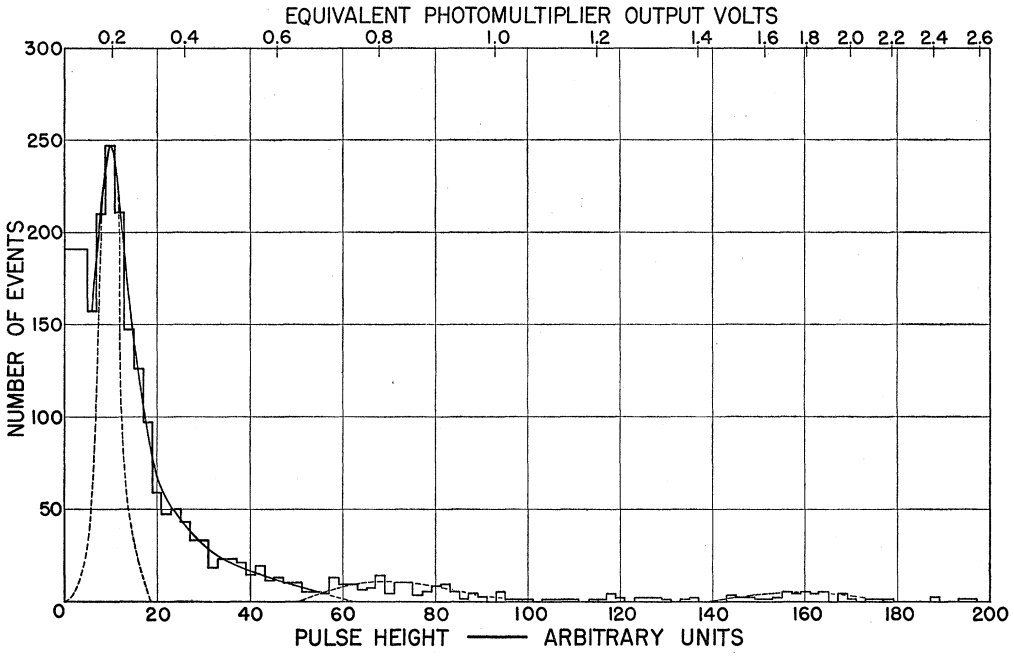

FIG. 10. Čerenkov pulse-height distribution for flight L, 0° direction, 27.6 g/cm² with wide scale, showing proton, He and Li peaks. Dotted curve is for sea-level mesons.

rapidly above the threshold that the determination of particle energy is not sensitive to the choice of what constitutes a minimum detectable pulse. The fill-in between the sea level and the high-altitude curves on the high side is to be associated with *nuclear* collisions, the electron collisions being already present in the sea-level curve. This effect is very pronounced, as would be expected for approximately 29 g/cm² of Lucite, or nearly half of a geometrical mean-free-path for protons. The Čerenkov effect comes from charged particles produced with $E/mc^2>0.34$ in the collisions. The multiplicity cannot be uniquely determined, as the residual path in the radiator is unknown for any particular event. Some of these pulses may be due to α particles or heavy nuclei of reduced velocity, but the principal contribution comes from nuclear collisions.

In Fig. 10 is shown the wide-range pulse-height distribution for flight L at 0° zenith. The singly charged peak is just resolved out of the width of the recording-oscilloscope background trace for this large scale (compare Fig. 9). There is a distinct peak at a voltage (read top scale) four times the singly charged peak, attributable to He, and a peak at nine times the singly-charged voltage attributable to Li. The latter is only two or three times background, so that the relative abundance figure is not very meaningful. However, we get the value H:He:Li=1:08:0.02 applicable at 27.6 g/cm² at $\lambda=40°$. The half-width of the He and Li peaks seems much smaller than the proton peak. Since all primaries have a value of E/mc^2 well up on the Čerenkov curve at this latitude, this is assumed to result from the improvement in photon statistics as the number of photons increases proportional to Z^2. For heavies, a nuclear collision may *decrease* or *increase* the output pulse, depending on the breakup of the heavy and the multiplicity of secondaries.

C. Azimuthal Data

The azimuthal data from the flights is summarized in Fig. 11. The counting rates were determined in each zenith position in ten azimuthal sectors. The relativistic data, as before, is plotted separately from the total telescope rate. The asymmetry effects are very pronounced even for the total radiation. For the total count at 60° zenith the E–W asymmetry is 30±5 percent, in agreement with that found previously at this latitude with Geiger telescopes.[1] For relativistic particles *only* the effect increases somewhat to about 35 percent. The E–W effect for pulses of He or larger size is not definite, as the statistics are quite poor in this case. The asymmetry at 120° zenith is not very well defined for the total radiation, but seems to bear the expected 180° phase relation to the 60° values.[18]

The largest effect occurs at 90° zenith if one considers *only* relativistic particles, i.e., those for which direction is established. The total count rate, being merely that of an ordinary Geiger telescope, shows *zero* effect at 90°. The analysis of the pulses giving Čerenkov radiation into the ten azimuthal sectors, however, shows an asymmetry of ≈80 percent at 90°. This measurement

[18] The gondola azimuth is referred to the telescope direction when pointing above the horizontal.

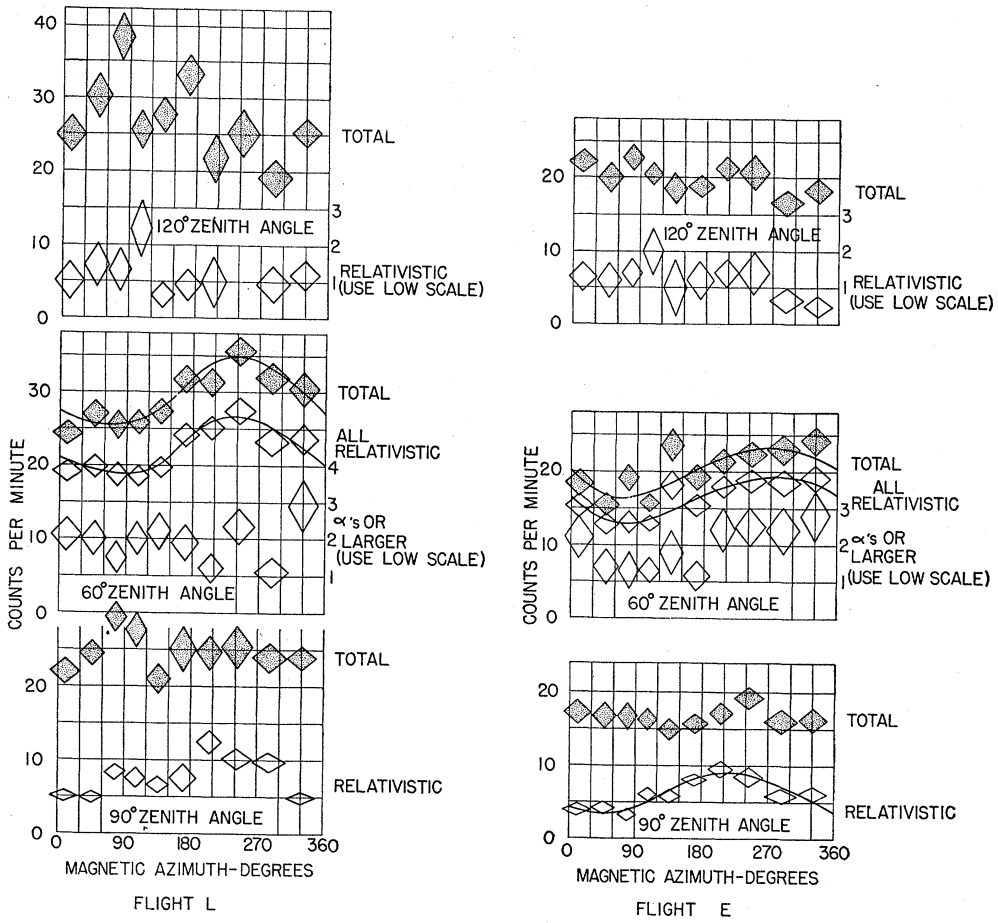

FIG. 11. Azimuthal data for flights E and L in 60°, 90°, and 120° zenith positions. The total and relativistic parts are plotted separately. At 60° zenith pulses ≥ 2 particles also are plotted.

in particular displays the great superiority of this type of detector over conventional telescopes for directional measurements.

Comparison between the observed azimuthal effect and the effect predicted from the primary spectrum and geomagnetic theory is shown in Figs. 12 and 13. The theoretical cut-off energy for protons at $\lambda=40°$ for 40° and 60° zenith angles as a function of azimuth is shown in Fig. 12. This comes from the work of Schremp,[19] who computed the shadow cone for this latitude, and from simple Störmer theory. The Störmer variable, as a function of zenith (z) and azimuth (φ), is given by the relation

$$r_0=\frac{\cos^2\lambda}{\gamma^2+(\gamma^2-\sin z\sin\varphi\cos^3\lambda)^{\frac{1}{2}}}. \qquad (3)$$

The value $\gamma=1.0$ at $\lambda=40°$ was used. Schremp's data are presented in the literature as projections of the allowed cone intersection with the unit hemisphere on the horizontal plane. From such figures the earth-shadow effect values were taken, with somewhat less accuracy than implied by the curves of Fig. 12. Figure 13 compares the predicted and observed curves for the azimuthal effect at $\lambda=40°$ for 60° and 90° zenith. The comparison was made as follows. The applicable integral number-energy spectrum obtained from the vertical flux at 15 g/cm² (see reference 1) is $0.30E^{-0.90}$/cm² sec sterad, with the energies in Bev of kinetic energy for protons. From this spectrum and the curves of Fig. 12 the curves of Fig. 13 were constructed. The counting rates from the present experiments were normalized to have the same azimuthal average as the predicted curves and plotted, with magnetic azimuth kept on an absolute basis. The flux values of the present measurements were on the average too high because of the somewhat larger atmospheric depth (25 *vs* 15 g/cm²), hence the normalization. Although the primary energy is expressed in Bev for protons, the comparison is valid for any type primary nucleus, except that all positive primaries are assumed. As shown in Fig. 13, the present results agree rather well with the Störmer theory at 60° zenith and are in definite disagreement

[19] E. J. Schremp, Phys. Rev. **54**, 153, 158 (1938).

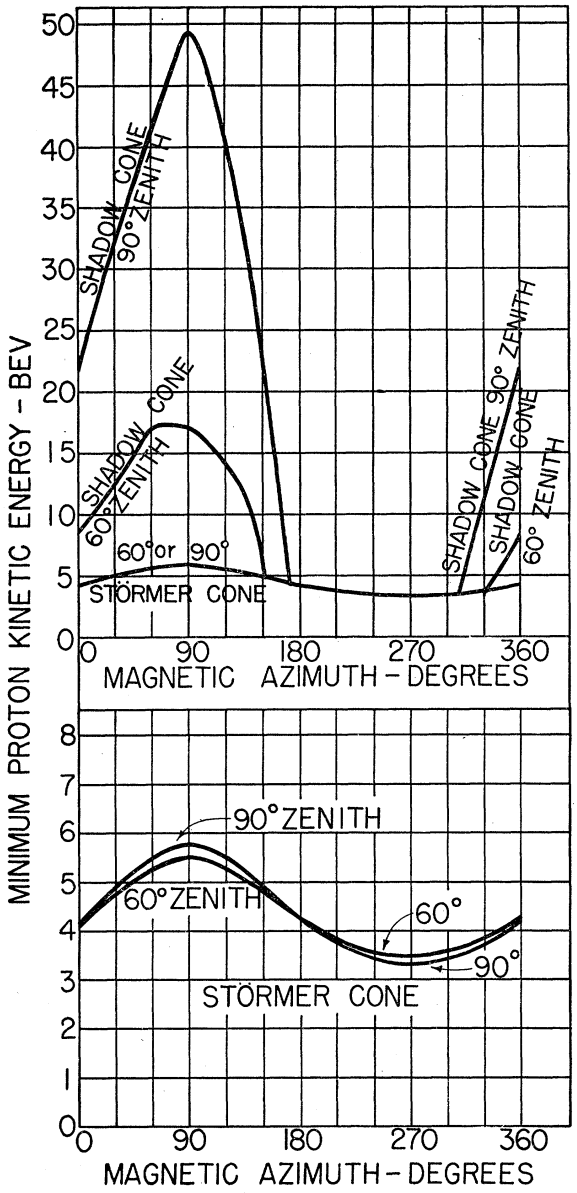

FIG. 12. Theoretical cut-off energy for $\lambda=40°$ considering Störmer theory (lower) and with the addition of the Schremp shadow cone calculation (above).

with the intensities predicted by the shadow-cone theory. At 90° zenith the present results lie *between* the simple Störmer and shadow-cone intensities. In the horizontal direction at 24 g/cm² there is 300 to 400 g/cm² of atmosphere ahead of the detector, so that the measurements are farther removed from the primaries. Nevertheless, the strong indication is that the shadow cones lie at somewhat larger zenith angles than predicted. Measurements at higher altitudes, say 5–6 g/cm², where large zenith-angle data are more meaningful, are essential to see if this conclusion is justified.

The albedo flux likely to affect ordinary Geiger telescopes is shown in Fig. 14, where the relativistic (Čerenkov-accompanied) events and the low-energy proton events are displayed as vector diagrams in the E–W plane. The upward relativistic flux is about 5 percent of the downward in any direction. For the low-energy protons, with direction undetermined, the intensity is 15–20 percent of the relativistic component. It is possible that a larger fraction of these are upward particles than for the relativistic case, but even in this case their number represents a low fraction of the total. Another group of particles are those with a range less than 30 g/cm² of Lucite, which are not detected at all. The large telescopes used formerly[1] to study the vertical and azimuthal effects between $\lambda=0°$ and $\lambda=40°$ contained 3 cm of Pb, which implied a minimum energy of 112 Mev for protons or 64 Mev for μ mesons. The Čerenkov data shows the splash albedo effects to be not more than 5 percent for the mesons, together with protons above 319 Mev. The telescopes included a group of protons between 112 and 319 Mev for which the splash albedo is not measured, but it is unlikely that a large fraction of these are upward moving, in view of the results for the energy range just above this, and their albedo contribution is hence small in relation

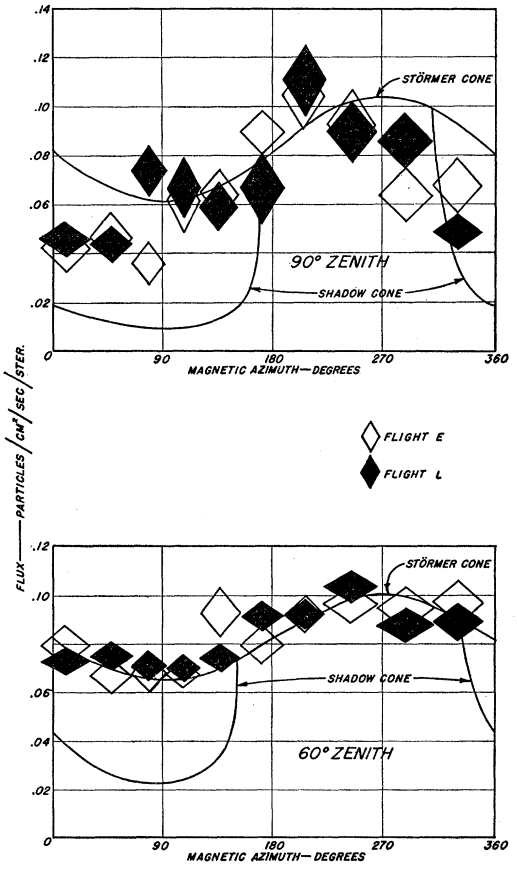

FIG. 13. Comparison of observed and predicted values of azimuthal effects at 60° and 90° zenith angles at $\lambda=40°$.

to the total flux. Therefore, the splash albedo values obtained, if applied to telescope experiments between $\lambda=0°$ and $\lambda=40°$, are too small by a factor of at least four to resolve the latitude-asymmetry disagreement.

Aside from its contribution to the splash albedo, which is probably small, the lower-energy proton flux is of interest even if 100 percent downward, as it affects the second discrepancy mentioned in the introduction, namely the absolute energy comparisons. Here we must consider the fraction of particles vertically detected at 15 g/cm² that are not primaries. The present data at ≈ 25 g/cm² show a flux that definitely contains at least 15 percent nonrelativistic protons which cannot be primaries. In addition, the relativistic counting rate is decreasing with decreasing depth between 27.6 and 23.6 g/cm² (see Table I), showing that part of this component may be secondaries as well. An extension of the present type of measurement to the highest obtainable altitude would be very useful in clarifying the situation. However, it appears that perhaps a 10–30 percent effect may be accounted for by such an investigation, but not a factor of two, as exists between the particle and ionization measurements of total energy.

It may now be stated in conclusion that neither the asymmetry discrepancy nor the energy balance discrepancy mentioned in the introduction can be explained by albedo effects at balloon altitudes at $\lambda=40°$.

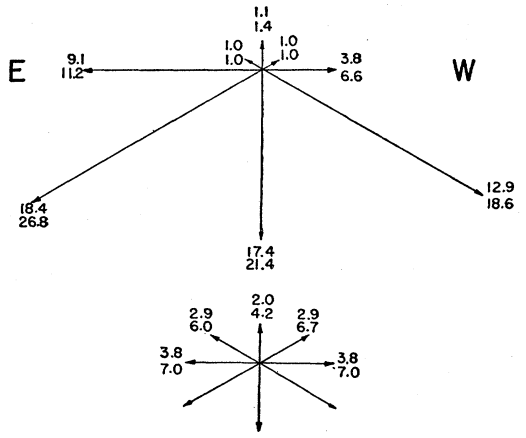

FIG. 14. Vector diagram in the E–W plane for relativistic particles (above) and protons of energy between 210 and 319 Mev (below). The upper numbers on each diagram refer to flight *E*, the lower to flight *L*. The values are in counts/minute. Statistical error ±10 percent. Flux (particles/cm² sec sterad) = (counts/min) × 0.009.

A possible alternative explanation for the low asymmetries observed at $\lambda=40°$ is suggested by the azimuthal effects measured with the Čerenkov detector which are free of splash albedo effects. This is the possibility that the shadow-cone limits lie at larger zenith angles than those predicted by Schremp's calculation.